Reactive & Functional Polymers 71 (2011) 849–856

Contents lists available at ScienceDirect

Reactive & Functional Polymers

journal homepage: www.elsevier.com/locate/react

Blue-emitting copolymers of isoquinoline and fluorene

Renchu Scaria [a], Nigel T. Lucas [b], Klaus Müllen [c], Josemon Jacob [a,*]

[a] *Centre for Polymer Science and Engineering, Indian Institute of Technology Delhi, Hauz Khas, New Delhi 110 016, India*
[b] *Department of Chemistry, University of Otago, Dunedin 9054, New Zealand*
[c] *Max Planck Institute for Polymer Research, Ackermannweg 10, 55128 Mainz, Germany*

ARTICLE INFO

Article history:
Received 3 March 2011
Received in revised form 10 May 2011
Accepted 12 May 2011
Available online 18 May 2011

Keywords:
Conjugated polymers
Polycations
Isoquinoline
N-alkylation
Solid-state packing

ABSTRACT

5,8-Linked copolymers of isoquinoline with fluorene were synthesized by Pd(0)-catalyzed Suzuki polycondensation reaction. The polymers showed good solubility in common organic solvents and the number average molecular weights determined from GPC analysis fall in the range of 7.03–8.08 × 10^3 g/mol. The photoluminescence spectra of these neutral materials in solution exhibit emission maxima in the range 408–426 nm. An X-ray diffraction study on a single crystal of a 5,8-di(9,9-dimethylfluoren-2-yl) isoquinoline model compound shows it to have a non-planar conformation and sheds light on the factors that drive the solid-state packing. The alkylation of the imine nitrogen was achieved by treatment with methyl iodide and the alkylated products were characterized by ^{1}H NMR, ^{13}C NMR and UV–vis spectroscopy. The absorption maxima of model compounds and polymers were red shifted by 46–70 nm upon *N*-alkylation.

1. Introduction

The optical and electronic properties of polymers containing *N*-heterocyclic moieties have been studied extensively for their potential use in organic light emitting diodes (OLEDs), organic solar cells and chemical sensors [1–4]. Quinoline, quinoxaline, oxadiazole and pyridine derivatives have been widely used as electron transporting/hole blocking materials in LED devices and LED blends because these types of units have excellent properties such as high electron affinity, high thermal and oxidation stability, and good charge injection [5–8]. Within the class of conjugated polymers, materials containing *N*-heterocyclic moieties have attracted considerable attention not only because of their electron-accepting abilities but also for the possibility of metal complexation, *N*-oxidation, *N*-protonation, and *N*-alkylation, leading to polymers with unique properties that are different from neutral polymers [4,9–14]. Recently, Swager and Izuhara have reported on a new class of nitrogen-containing polyheterocycles with high electron affinity [15,16]. Polyquinolines have been widely studied as *n*-type semiconductors and emissive materials in electronic devices [17–22]. Compared to quinoline based materials, there have been limited reports on materials derived on isoquinoline for electronic applications [23–26]. Recently, isoquinoline based metal complexes have been studied for their potential application in phosphorescence-based organic and polymeric light-emitting devices [27–29]. Apart from a few reports on polyisoquinolines, synthesis and opto-electronic properties of oligomers or polymers bearing isoquinoline moieties with a 5,8-linkage in the conjugated backbone have not yet been explored. In this contribution, the synthesis, characterization and optical studies of model compounds and copolymers derived from isoquinoline and dialkylfluorene have been investigated. Oligo- and polyfluorenes have emerged as the most attractive blue-emitting materials due to their high efficiency and good thermal stability of polymers [30–37]. Combining the electron affinity of isoquinoline and blue light-emitting nature of highly soluble polyfluorenes, the copolymers are expected to possess good solubility, thermal stability and blue light-emitting properties. The absorption maxima of neutral polymers can be extended by introduction of cations into the polymer backbone. In a previous study, we reported on the synthesis of conjugated polyfluorenyl cations and the control of cation density and solubility by copolymerization [38]. In the case of isoquinoline based materials, the presence of an electron deficient nitrogen atom offers the possibility to tune the optical properties by *N*-alkylation. *N*-alkylation is widely investigated as a means to tailor the optical properties of polyquinoline and polypyridine derivatives. The *N*-alkylated polymers bearing cations in the backbone have exhibited a red shift in absorption maxima as compared to their neutral polymers [13,34,39]. Isoquinoline with different linkage positions offers the possibility to synthesize novel organic materials with tunable optical properties. In this study, copolymers and model compounds of 5,8-linked isoquinoline with fluorene have been prepared, their optical and thermal properties investigated, and the solid-state structure of a model compound

---

* Corresponding author. Tel.: +91 9911061890; fax: +91 11 2659 1421.
E-mail address: jacob@polymers.iitd.ac.in (J. Jacob).

1381-5148/$ - see front matter © 2011 Elsevier Ltd. All rights reserved.
doi:10.1016/j.reactfunctpolym.2011.05.006

determined. In addition, conjugated polycations formed by *N*-alkylation of the isoquinoline unit are discussed.

2. Experimental

2.1. Materials

Dry solvents, stored in a glove box, were used for specified reactions. 5,8-dibromoisoquinoline (**2**) and 5-bromoisoquinoline (**3**) were synthesized according to literature procedures [40]. 9,9-Dimethylfluorene-2-(4,4,5,5-tetramethyl-[1,3,2]-dioxaborolane) (**4**), 2,7-bis(4,4,5,5-tetramethyl-[1,3,2]-dioxaborolane)-9,9-dimethylfluorene (**5**), 2,7-bis(4,4,5,5-tetramethyl-[1,3,2]-dioxaboralan-2-yl)-9,9-dioctylfluorene (**8a**) and 2,7-bis(4,4,5,5-tetramethy-[1,3,2]-dioxaboralan-2-yl)-9,9-bis(2-ethylhexyl)fluorene **(8b)** were also synthesized in accordance with literature procedures [41–44].

2.2. Characterization

^{1}H and ^{13}C NMR spectra were recorded on a Bruker 300 MHz spectrometer operating respectively at 300 MHz for ^{1}H and 75 MHz for ^{13}C NMR using deuterated solvents with tetramethylsilane (TMS) as a reference. UV–vis absorption spectra were recorded in THF solution on a Perkin-Elmer Lambda 25 Spectrophotometer. Photoluminescence measurements were carried out with a Fluorolog HORIBAJOBIN YVON spectrophotometer using a xenon-arc lamp as a source, in THF solution. Thermal degradation was studied by TGA on a Perkin Elmer Pyris 7 thermal analysis system under a dynamic atmosphere of nitrogen at a heating rate of 20 °C/min. Differential scanning calorimetry (DSC) data were recorded using a TA DSC Q200 calibrated with indium at heating/cooling rates of 10 °C min^{-1} under nitrogen. The molecular weights of the polymers were determined by Gel Permeation Chromatography against polystyrene standard in THF at 30 °C. The cyclic voltammetric studies were conducted on an Autolab 30, Potentiostat/Galvanostat at a constant scan rate of 20 mV s^{-1}. Platinum wires were used as both the counter and working electrodes, and Ag/AgCl electrode was used as the reference electrode. Thin films of copolymers **9a** and **9b** on platinum electrodes were prepared by dipping the electrode into a 0.5–1.0 wt.% copolymer solution in toluene. The resulting films were dried in a vacuum oven at 80 °C. Cyclic voltammogram of **12a** and **12b** were taken from a solution of corresponding compounds in 0.1 M tetrabutylammonium tetrafluoroborate ($TBABF_4$) in acetonitrile, which was used as the electrolyte.

2.3. Synthesis of model compounds

2.3.1. Synthesis of 5,8-di(9,9-dimethylfluoren-2-yl) isoquinoline (**6**)

5,8-dibromoisoquinoline **2** (0.25 g, 0.87 mmol), 9,9-dimethyl fluorene-2-(4,4,5,5-tetramethyl-1,3,2-dioxaborolane) **4** (0.84 g, 2.63 mmol), 2 M K_2CO_3 (2.6 mL, 5.22 mmol) were added to 5 mL of 1,4-dioxane in a Schlenk flask. The solution was purged with N_2 for 15 min, and then $Pd(PPh_3)_4$ (0.06 g, 2 mol%) was added. The reaction mixture was heated with stirring at 100 °C. The reaction was followed by TLC and after 20 h was worked up. The cooled reaction mixture was extracted into chloroform and the organic layer was washed with brine and then dried over anhydrous Na_2SO_4. The solvent was removed under vacuum and the residue was purified by column chromatography over silica gel with 0–10% ethyl acetate in hexane as the eluent, to give **6** as a white solid (0.32 g, 71%). ^{1}H NMR (300 MHz, $CDCl_3$): $\delta = 9.47$ (s, 1H), 8.45 (d, 1H, $J = 6$ Hz), 7.88 (m, 3H), 7.83–7.79 (m, 3H), 7.70 (d, 1H, $J = 7.2$ Hz), 7.64 (s, 1H), 7.59–7.49 (m, 5H), 7.39–7.35 (m, 4H). ^{13}C NMR (75 MHz): $\delta = 154.03$, 153.96, 153.85, 151.61, 143.04, 140.78, 139.06, 138.91, 138.66, 138.01, 137.64, 134.73, 130.50, 129.10, 128.89, 127.87, 127.53, 127.10, 124.46, 124.25, 122.66, 120.19, 120.03, 118.71, 47.01, 27.19.

2.3.2. Synthesis of 2,7-di(isoquinol-5-yl)-9,9-dimethylfluorene (**7**)

In a Schlenk flask, 5-bromoisoquinoline **3** (0.28 g, 0.63 mmol), 2,7-bis(4,4,5,5-tetramethyl-[1,3,2]dioxaborolane)-9,9-dimethylfluorene **5** (0.46 g, 2.20 mmol), 2 M K_2CO_3 (4.6 mL, 9.19 mmol) and 6 mL of 1,4-dioxane were taken and purged with N_2 for 15 min. Then, $Pd(PPh_3)_4$ (0.06 g, 2 mol%) was added and the reaction mixture was heated with stirring at 100 °C for 20 h. The cooled reaction mixture was extracted into chloroform and the organic layer was washed with brine and then dried over anhydrous Na_2SO_4. The solvent was removed under vacuum and the residue was purified by column chromatography over silica gel with 0–20% ethyl acetate in hexane as the eluent, to give **7** as a yellow solid (0.15 g, 53%). ^{1}H NMR (300 MHz, $CDCl_3$): $\delta = 9.34$ (s, 2H), 8.54 (d, 2H, $J = 5.7$ Hz), 8.04 (d, 2H, $J = 8.1$ Hz), 7.94 (d, 2H, $J = 7.8$ Hz), 7.85 (d, 2H, $J = 5.7$ Hz), 7.79 (d, 2H, $J = 6.9$ Hz), 7.73 (t, 2H, $J = 7.35$ Hz), 7.59 (s, 2H), 7.53 (d, 2H, $J = 7.5$ Hz). ^{13}C NMR (75 MHz): $\delta = 154.24$, 152.92, 143.42, 139.49, 138.35, 138.26, 134.18, 130.96, 129.02, 127.11, 126.82, 124.26, 120.19, 118.54, 47.16, 27.21.

2.4. Synthesis of polymers

2.4.1. Synthesis of ***9a***

A mixture of 5,8-dibromoisoquinoline **2** (0.25 g, 0.87 mmol), 2,7-bis(4,4,5,5-tetramethyl-1,3,2-dioxaboralan-2-yl)-9,9-dioctylfluorene **8a** (0.56 g, 0.87 mmol) and $Pd(PPh_3)_4$ (0.020 mg, 2 mol%) were added to a degassed mixture of toluene (3 mL), Aliquat 336 (3 drops) and 1.7 mL of 2 M Na_2CO_3. The mixture was vigorously stirred at 85 °C for 48 h under a nitrogen atmosphere. Then, bromobenzene (45 µL, 0.43 mmol) was added as an end capping agent to the mixture and heated for an additional 12 h. After cooling to room temperature, the viscous solution was poured into 300 mL of methanol. The precipitated polymer was isolated by filtration. It was further purified by Soxhlet extraction with acetone followed by reprecipitation from methanol. The polymer was dried under reduced pressure to yield **9a** as a pale yellow solid (0.36 g, 80%). ^{1}H NMR (300 MHz, $CDCl_3$): $\delta = 9.51$ (s, 1H), 8.57 (d, 1H), 7.99–7.89 (4H, br), 7.74 (s, 1H), 7.62–7.59 (5H, br), 2.11 (4H, br), 1.17–0.82 (m, 30H, br). UV–vis (THF) λ_{max}: 358 nm, GPC: $M_n = 8.08 \times 10^3$ g/mol, PDI = 2.85.

2.4.2. Synthesis of ***9b***

A mixture of 5,8-dibromoisoqunoline **2** (0.26 g, 0.90 mmol), 2,7-bis(4,4,5,5-tetramethy-1,3,2-dioxaboralan-2-yl)-9,9-bis(2-ethylhexyl) fluorene **8b** (0.58 g, 0.90 mmol) and $Pd(PPh_3)_4$ (0.021 mg, 2 mol%) were added to a degassed solution of toluene (3 mL), Aliquat 336 (three drops) and 1.8 mL of 2 M Na_2CO_3. The mixture was stirred vigorously at 85 °C for 48 h. Bromobenzene (47 µL, 0.45 mmol) was then added as end capping agent to the mixture and further heated for 12 h with stirring. The reaction mixture was cooled to room temperature and the viscous solution poured into 300 mL of methanol. The precipitated polymer was isolated by filtration and purified by Soxhlet extraction with acetone followed by reprecipitation from methanol. The polymer was dried under reduced pressure to give **9b** in 78% yield (0.36 g). ^{1}H NMR (300 MHz, $CDCl_3$): $\delta = 9.53$ (s, 1H), 8.55 (d, 1H), 7.97–7.60 (m, 9H), 2.13 (t br, 4H), 1.00–0.66 (m br, 30H). UV–vis (THF) λ_{max}: 354 nm, GPC: $M_n = 7.03 \times 10^3$ g/mol, PDI = 3.04.

2.5. Synthesis and characterization of isoquinolinium salts

2.5.1. Synthesis of **10**

Iodomethane (0.049 mL, 0.77 mmol) was added dropwise to 5,8-di(9,9-dimethylfluoren-2-yl)isoquinoline **6** (0.050 g, 9.74×10^{-2} mmol) dissolved in 7 mL of chloroform. The reaction mixture was stirred at room temperature for 24 h and the yellow solution was extracted with dichloromethane to yield **10** as an yellow solid (0.062 g, 96%). ^{1}H NMR (300 MHz, $CDCl_3$): δ = 9.32 (s, 1H), 9.02 (d, 1H, 6.3 Hz), 8.42 (d, 1H, 6.3 Hz), 8.12 (d, 1H, 7.5 Hz), 7.96 (t, 2H, 8.1 Hz), 7.85 (d, 1H, 7.8 Hz), 7.76–7.67 (m, 3H), 7.62 (d, 1H, *J* = 7.5 Hz), 7.5 (s, 1H), 7.41–7.34 (m, 7H), 4.71 (s, 3H), 1.73 (s, 6H). ^{13}C NMR (75Mz, $CDCl_3$) δ = 154.85, 154.59, 153.93, 153.77, 148.42, 143.15, 140.44, 139.99, 139.66, 138.03, 136.40, 135.94, 135.15, 134.41, 131.46, 129.66, 128.82, 127.97, 127.13, 126.73, 124.75, 124.51, 124.01, 122.64, 120.81, 120.48, 49.89, 47.16, 27.07.

2.5.2. Synthesis of **11**

To 2,7-di(isoquinol-5-yl)-9,9-dimethylfluorene **7** (0.050 g, 0.011 mmol) dissolved in 7 mL of chloroform, iodomethane (0.055 mL, 0.88 mmol) was added. The reaction mixture was stirred at room temperature for 24 h to yield an orange precipitate which is washed with chloroform to yield **11** as an orange solid (0.065 g, 98%). ^{1}H NMR (300 MHz, DMSO-*d6*): δ = 10.09 (s, 2H), 8.67 (d, 2H, *J* = 6.3 Hz), 8.54 (d, 2H, *J* = 7.8 Hz), 8.35–8.29 (m, 6 H), 8.18–8.14 (m, 4H), 7.61(d, 2H, *J* = 7.5 Hz), 4.50 (s, 6H), 1.59 (s, 6H). ^{13}C NMR (75 MHz, DMSO-d_6): δ = 154.59, 151.02, 139.36, 138.32, 137.06, 136.31, 131.01, 129.83, 129.16, 127.74, 124.50, 123.39, 121.17, 47.84, 47.13, 26.72.

2.5.3. Synthesis of **12a**

Iodomethane (0.12 mL, 1.93 mmol) was added dropwise to **9a** (0.125 g, 2.414×10^{-4} mol of monomer) in 6 mL of chloroform. The reaction mixture was stirred at room temperature for 24 h to yield a red precipitate which is washed with chloroform to yield **12a** as a red solid (0.120 g, 75%). ^{1}H NMR (300 MHz, DMSO-d_6): δ = 9.68 (s br, 1H), 8.79 (d br, 1H), 8.40–7.71 (m br, 9H), 4.54 (s, 3H), 2.21 (t br, 4H), 1.13 – 0.78 (m br, 30H).

2.5.4. Synthesis of **12b**

Iodomethane (0.12 mL, 1.93 mmol) was added dropwise to **9b** (0.125 g, 2.41×10^{-4} mol of monomer) in 6 mL of chloroform. The reaction mixture was stirred at room temperature for 24 h to yield a red precipitate which is washed with chloroform to yield **12b** as a red solid (0.120 g, 75%). ^{1}H NMR (300 MHz, DMSO-*d6*): δ = 9.59 (s, 1H, br), 8.86 (d, 1H, br), 8.32–7.70 (m, 9H, br), 4.54 (s, 3H), 2.24 (t, 4H, br), 0.91–0.62 (m, 30H, br).

2.6. X-ray crystallography

Data were collected at 91 K with ω and φ scans to 50.78° 2θ on a Bruker Kappa X8 diffractometer with APEX II detector, and employing graphite monochromated Mo Kα radiation generated from a fine-focus sealed tube. The data integration and reduction were undertaken with SAINT and XPREP (Bruker Analytical X-ray Instruments Inc, Madison, Wisconsin, USA, 1995) and subsequent computations were carried out with the Xseed graphical interface to SHELX97 [45]. A Gaussian absorption correction was applied to the data [46]. The structure was solved in the monoclinic space group $P2_1/c$ (#14) by direct methods with SHELXS-97 [45], then extended and refined with SHELXL-97. The non-hydrogen atoms in the asymmetric unit were modelled with anisotropic displacement parameters. A riding atom model with group displacement parameters was used for the hydrogen atoms, with the exception of the chloroform hydrogen atom, which was fully refined to investigate its interaction with the isoquinoline nitrogen atom.

3. Results and discussion

3.1. Synthesis and characterization of model compounds and polymers

Scheme 1 outlines the synthetic scheme for model compounds and polymers made by the Suzuki coupling reaction. Coupling of **2** and **4** in a mixture of dioxane and aqueous K_2CO_3 solution gave 5,8-di(9,9-dimethylfluoren-2-yl)isoquinoline (**6**) in 71% yield. In a similar manner, the coupling of **3** and **5** gave 2,7-di(isoquinol-5-yl)-9,9-dimethylfluorene (**7**) in 53% yield. The reaction of **2** with 2,7-bis(4,4,5,5-tetramethy-1,3,2 dioxaboralan-2-yl)-9,9-dioctylfluorene **(8a)** under Suzuki polymerization conditions furnished **9a** in 80% yield with a degree of polymerization (P_n) of 15 and a polydispersity (M_w/M_n, PDI) of 2.85. **9b** was obtained by reaction of **2** with 2,7-bis(4,4,5,5-tetramethy-[1,3,2]-dioxaboralan-2-yl)-9,9-bis(2-ethylhexyl)fluorene **(8b)** under identical conditions in 82% yield with a P_n of 13 and a PDI of 3.05. Although the measured PDI is slightly higher than normal, repeated Soxhelt extraction and reprecipitation did not improve the PDI of the copolymers. We believe the molecular weights can be further improved by use of alkyl chains with longer solubilising groups and will be reported separately. The compounds **6** and **7** and the polymers **9a** and **9b** show good solubility in common organic solvents.

The molecular structure of the polymers and model compounds were confirmed by ^{1}H NMR spectroscopy. In **9b** the orientation of isoquinoline units in the polymer chain are random with respect to each other, as evidenced from their ^{1}H NMR spectra. In the case of model compound **6**, a single crystal was subjected to X-ray diffraction analysis enabling insight into the molecular confirmation and solid state organization of the molecule. The thermal properties of the polymers were determined by DSC and TGA measurements. The degradation temperature of polymers at 5% weight loss (T_d) was in the range of 408–438 °C. The glass transition temperatures (T_g) of **9a** and **9b** are 91 °C and 95 °C, respectively. The physical properties of polymers are summarized in Table 1.

3.2. Optical properties of model compounds and polymers

In order to study the optical properties of polymers and model compounds, UV–vis spectra were recorded in THF solution, which are depicted in Fig. 1. When isoquinoline is end-capped at 5,8 positions with fluorene units (**6**), the absorbance maximum is observed at 340 nm. On the other hand, when fluorene is end-capped with an isoquinoline unit at both ends (**7**), the absorbance maximum is observed at 327 nm. The observed trend is in accordance with what is expected as **7** has lower conjugation length compared to **6**. Also, the extent of conjugation between neighbouring fluorene and isoquinoline units will largely depend on the twist angle. The absorption maxima of **9a** and **9b** are at 358 nm and 354 nm, respectively.

The photoluminescence spectra of the model compounds and polymers were recorded in THF and are shown in Fig. 2. When fluorene is end capped with isoquinoline units on either side, the emission maximum is observed at 408 nm. However, when isoquinoline is end caped at 5,8-positions with fluorene units, the emission maximum is at 424 nm. The observed Stokes shifts for **6** and **7** are 84 nm and 81 nm, respectively. Polymers **9a** and **9b** show emission maxima at 417 nm and 426 nm giving Stokes shifts of 59 nm and 72 nm respectively. The magnitude of Stokes shift in conjugated systems describes the structure reorganization between the ground and excited states and/or energy migration to minority segments having greater conjugation lengths [47]. The smaller Stokes shift of the polymers compared to model compounds indicates the larger structure reorganization (bond twisting, solution relaxation or change in electronic structure)

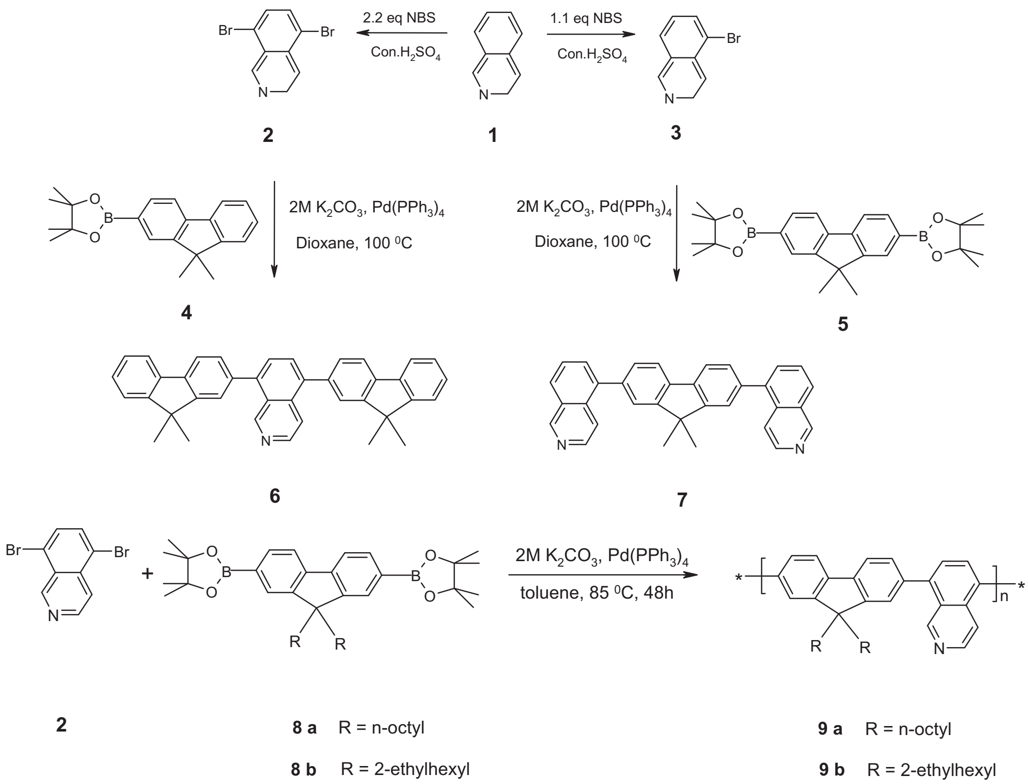

Scheme 1. Synthetic scheme for model compounds and polymers.

involved in the latter case. The photophysical properties of polymers and model compounds are summarized in Table 2.

3.3. Solid state structure of the neutral model compound **6**

Slow diffusion of methanol into a chloroform solution of 5,8-di(9,9-dimethylfluoren-2-yl)isoquinoline (**6**) yielded needle-like crystals, one of which was subjected to X-ray diffraction structure analysis (Fig. 3). The compound crystallized as a 1:1 chloroform adduct with four molecules of each per unit cell in the centrosymmetric $P2_1/c$ space group. Attempts to obtain single

Table 1
Physical properties of polymers.

Polymer	Yield (%)	$M_n \times 10^3$(g/mol)[a]	M_w/M_n[a]	T_d (°C)[b]	T_g (°C)[c]
9a	80	8.08	2.85	424	91
9b	78	7.03	3.04	403	95

[a] Number–average molecular weight (M_n) and polydispersity index (M_w/M_n) determined by means of GPC in THF on the basis of polystyrene calibration.

[b] Degradation temperature at 5% weight loss (T_d) measured by TGA at a heating rate of 20 °C/min under N_2 atmosphere.

[c] Glass transition temperature measured by DSC at a heating rate of 10 °C/min under N_2 atmosphere.

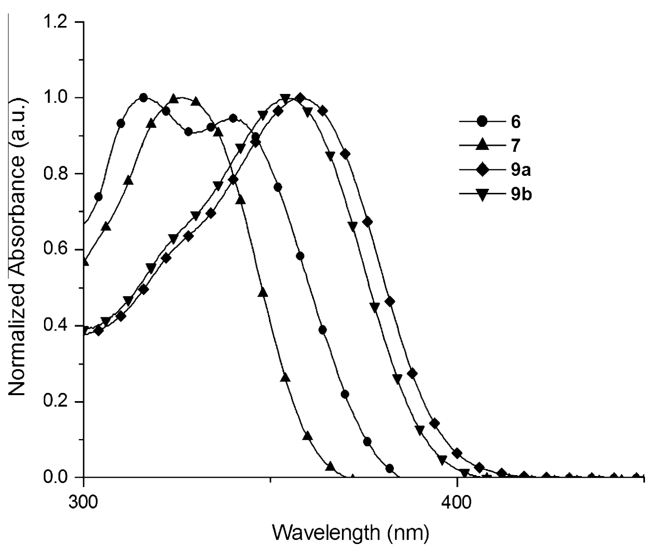

Fig. 1. UV–vis spectra of model compounds and polymers in THF solution.

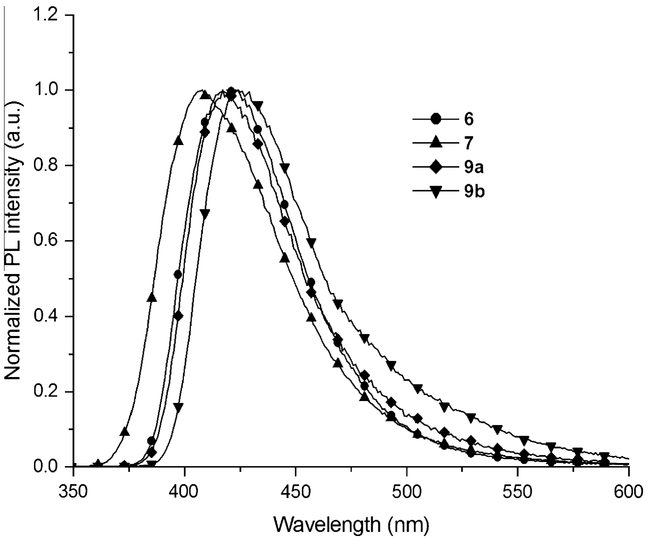

Fig. 2. Photoluminescence spectra of model compounds and polymers in THF solution.

Table 2
Photophysical properties of polymers and model compounds.

Polymer/model compound	λ_{max} (nm)[a]	λ_{em} (nm)[b]
9a	358	417
9b	354	426
6	340	424
7	327	408

[a] UV–vis absorption maxima recorded in THF solution.
[b] Photoluminescence emission maxima recorded in THF solution.

crystals of **6** were only successful using chloroform and the study confirms that the solvent plays an active role in the crystallization. The unsaturated core of **6** adopts a non-planar conformation, with dihedral angles of 52.6° (C5–C12) and 67.3° (C8–C32) between the isoquinoline and respective fluorene units. All bond lengths and angles are within the usual ranges expected. Few other 5- or 8-substituted isoquinolines have been structurally characterized [48–51]; this is the first example of a structurally characterized 5,8-diaryl substituted isoquinoline.

The crystal packing provides insight into how this type of molecule may organize within the thin films typically needed in optoelectronic devices. Tightly-packed sheets of **6**, stacked along the *a*-axis, display face-to-face π-stacking between pairs of isoquinoline units (separation 3.52 Å) and several C–H···C(π) interactions involving fluorene moiety hydrogens (C14–H14···C43 2.83 Å, C24–H24a···C34 2.86 Å, C36–H36···C3 2.86 Å, C44–H44a···C6 2.89 Å) (Fig. 4). Further stabilization of the structure arises from C11–H11···N interactions (2.71 Å) within the inversion-related pairs. The layers of **6** are separated by chloroform molecules which appear to interact strongly with the isoquinoline nitrogen through a Cl_3C–H···N hydrogen bond (2.27 Å; C–H–N 158.8°), but isolate the layers of **6** from one another. Nevertheless, the aforementioned combination of close intermolecular contacts results in good interaction between the molecules of **6** within the *b*–*c* planes of the crystal.

3.4. Synthesis and characterization of isoquinolininum salts

Reaction of the neutral model compounds and polymers with iodomethane generated the corresponding isoquinolininum salts. Alkylation induced a change in solution color from colorless to yellow. The formation of cations is evidenced by significant shift in signals in ^{1}H NMR spectra, along with the presence of a new peak at around 4.5 ppm due to N-CH_3 protons. As examples, the ^{1}H NMR spectra of **9b** and **12b** are given in Figs. 5 and 6, respectively.

The degree of methylation can be determined by peak ratios of *N*-methyl protons and aromatic protons, which indicates complete conversion to the cationic form. The resulting structures of cations are given in Chart 1. Compound **10** is soluble in chloroform, but the other materials show good solubility only in polar solvents such as dimethyl sulphoxide (DMSO) and N,N-dimethylformamide (DMF).

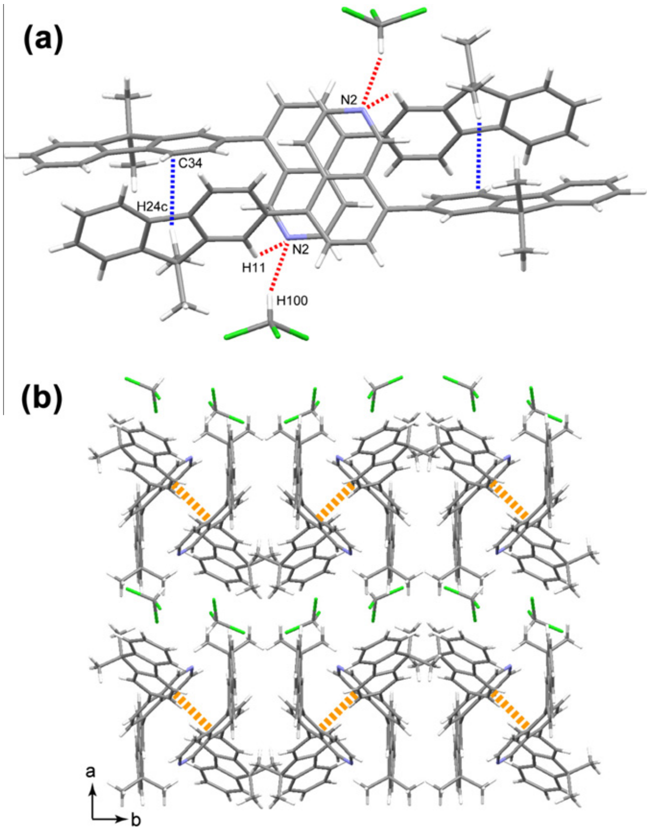

Fig. 4. Crystal structure packing diagrams of **6**·$CHCl_3$, (a) showing inversion-related pairs with short C–H···N contacts (red) involving a fluorene and chloroform, and C–H···C(π) intermolecular close contacts between fluorenes (blue). Note the π-stacking overlap of the isoquinoline fragments, as viewed from above; (b) packing diagram, as viewed along the *c*-axis, showing two layers of **6** separated by chloroform molecules. Interlayer π-stacking of the isoquinoline fragments is highlighted with orange dotted lines. (For interpretation of the references to color in this figure legend, the reader is referred to the web version of this article.)

3.5. Cyclic Voltammetric Studies

Cyclic voltammetry (CV) was performed to estimate the highest occupied molecular orbital (HOMO) and lowest unoccupied molecular orbital (LUMO) energy levels of the synthesized polymers. The HOMO levels of the polymers were calculated from the onset oxidation potential according to the equation HOMO = $-e(E_{ox} + 4.4)$ eV [52]. The LUMO levels of the polymers were determined by subtraction of the band gap energy (E_g) from the HOMO energy level following LUMO = HOMO – E_g. The optical band gaps (E_g) were calculated from the absorption edge of the copolymer films. The results of the electrochemical measurements are summarized in Table 3.

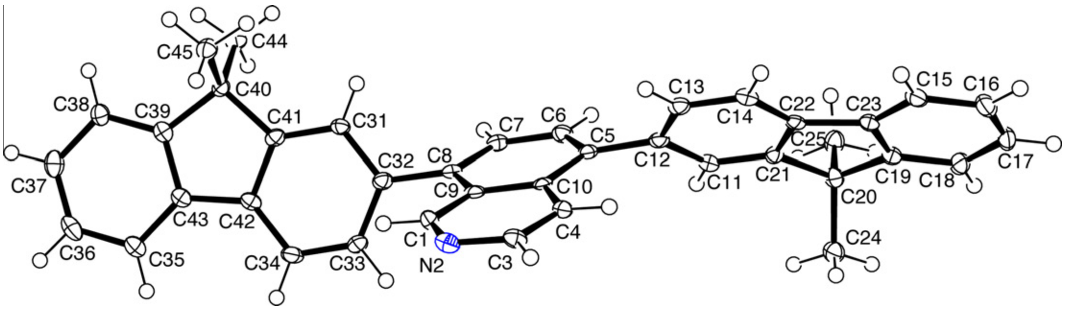

Fig. 3. ORTEP representation of a crystal structure of **6**·$CHCl_3$ showing the numbering scheme. The chloroform solvate molecule has been omitted for clarity. Displacement ellipsoids are depicted at 50% probability.

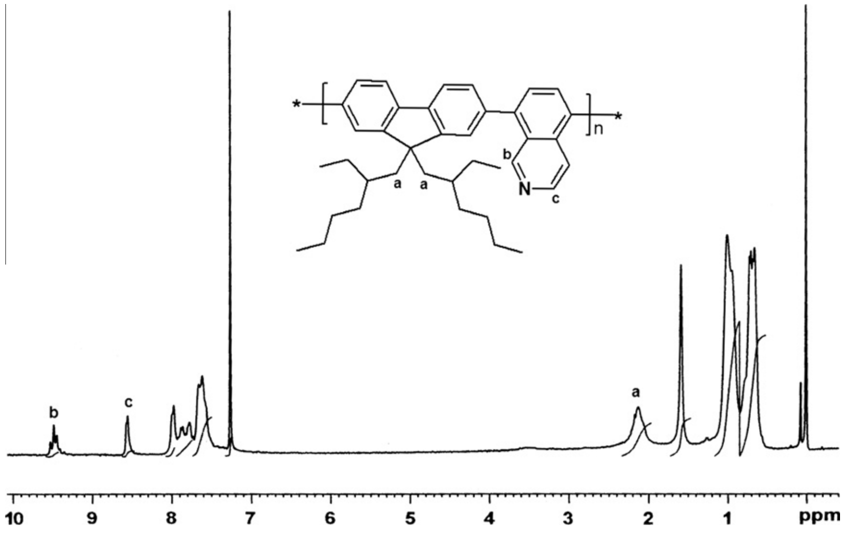

Fig. 5. ^{1}H NMR spectrum of **9b** in $CDCl_3$ solution.

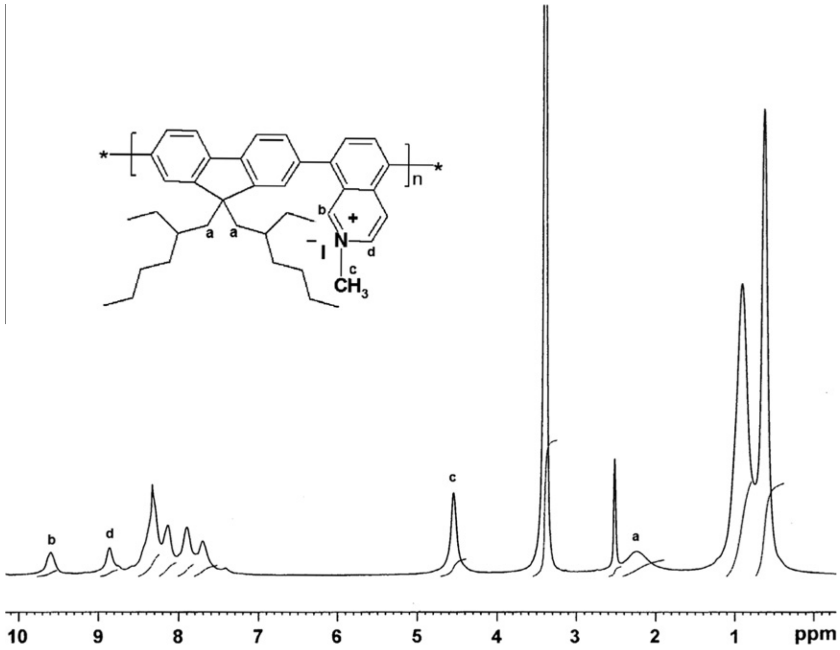

Fig. 6. ^{1}H NMR spectrum of **12b** in d_6-DMSO.

On the basis of roughly evaluated oxidation potentials, the HOMO levels of **9a** and **9b** was estimated as −5.94 and −5.95 eV respectively. The LUMO energy levels of **9a** and **9b** are −2.89 and −2.96 eV respectively. The HOMO energy levels of **12a** and **12b** are −5.98 and −5.99 eV, and their LUMO energy levels are −3.52 and −3.55 eV respectively. Upon *N*-methylation, the HOMO energy levels of polymers **9a** and **9b** are lowered by 0.04 eV, while the LUMO energy levels are lowered by 0.63 and 0.59 eV respectively. Thus, the formation of positive charge on the ring nitrogen by methylation lowered the energy levels of both HOMO and LUMO.

3.6. Optical properties of isoquinolininum salts

In order to study the effect of *N*-alkylation on the optical properties, the conjugated cations were generated by *N*-alkylation from the precursor materials by treatment with methyl iodide. The UV–vis spectra of the cationic model compounds and polymers in DMF solution are depicted in Fig. 7.

The absorption spectra of the polycations reveal a new wavelength absorption band approximately around 400 nm. The new absorption band probably originates from optical transition involving charge transfer from dialkyl fluorene moieties to positively charged nitrogen centre of isoquinoline residue. The polycations **12a** and **12b** have λ_{max} of 404 nm and 405 nm respectively. The cations **10** and **11** generated by *N*-alkylation of the precursor model compounds show λ_{max} values of 392 nm and 397 nm, respectively. Thus, upon cation formation the absorption maxima are significantly red shifted compared to their neutral compounds. The formation of a positive charge on the nitrogen atom by *N*-methylation lowered the energy of both HOMO and LUMO orbitals. However, presence of the greater amount of electron density on the nitrogen in the LUMO lowered its energy more than that of the HOMO; therefore, the optical band gap decreases, resulting

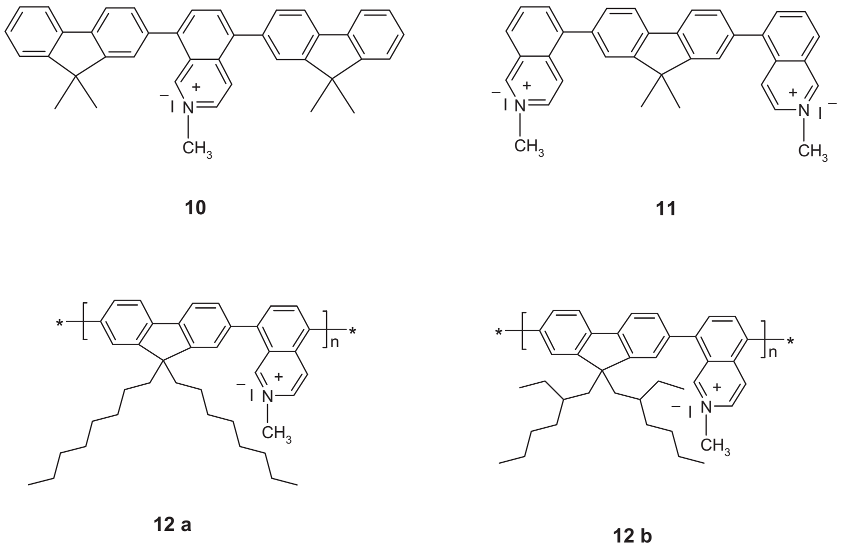

10 **11** **12 a** **12 b**

Chart 1. Isoquinolinium salts of the model compounds and polymers.

Table 3
Electrochemical properties of polymers.

Polymers	E_{ox} (V)	E_g^{opt} (eV)[a]	HOMO (eV)[b]	LUMO (eV)[c]
9a	1.54	3.05	−5.94	−2.89
9b	1.55	2.99	−5.95	−2.96
12a	1.58	2.46	−5.98	−3.52
12b	1.59	2.44	−5.99	−3.55

[a] Optical band gap, calculated from the absorption edge of the copolymer films, $E_g = 1240/\lambda_{\mathrm{edge}}$.
[b] Determined from the onset oxidation potential. HOMO = $-e(E_{ox} + 4.4)$ eV;
[c] LUMO = (HOMO − E_g) eV.

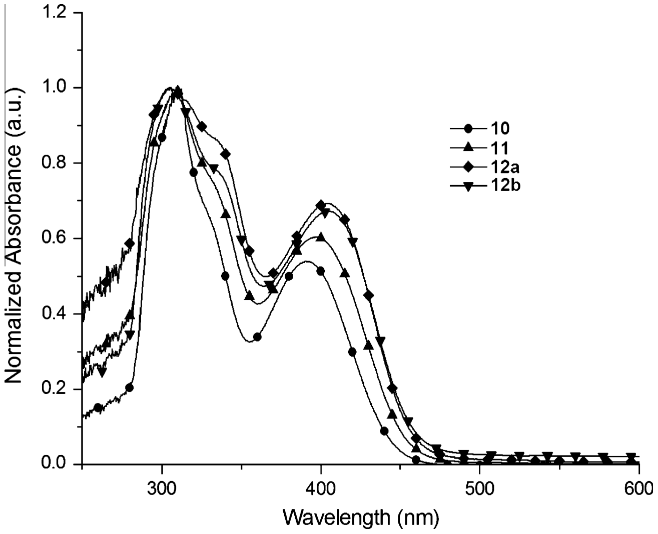

Fig. 7. UV–vis spectra of isoquinolininum salts in DMF solution.

in the longer wavelength absorption [53]. It should be noted that a red shifted absorbance along with appearance of new absorption band was observed when poly(*para*-pyridylvinylene)s were *N*-alkylated with methyl triflate [39]. In the case of **9a** and **9b**, the red shift upon conversion to cationic forms **12a** and **12b** is 46 nm and 51 nm, respectively, while in the case of model compounds **6** and **7**, conversion to cationic forms **10** and **11** red shifted the absorption maxima by 52 nm and 70 nm, respectively. Among the model compounds, the significantly larger red shift in the absorption maximum in the case of **11** compared to **10** is due to the presence two *N*-alkylated isoquinoline moieties in the former. The structural changes induced by *N*-alkylation could also affect the extent of conjugation between neighbouring fluorene units and isoquinoline units causing a large variation in absorption maxima.

The photoluminescence (PL) quantum yields of the polymers in solution were investigated by using anthracene ($\Phi_{\mathrm{PL}} = 0.27$) as a standard [54]. The PL quantum yields of **9a** and **9b** in THF solution are 0.84 and 0.62 respectively and that of **12a** and **12b** in ethanol solution are 0.07 and 0.10 respectively. In general, the charge transfer process is non emissive or weakly fluorescent and competes with fluorescence [55]. Thus, *N*-alkylation results in lower quantum yields compared to neutral polymers.

4. Conclusions

In conclusion, a new series of isoquinoline based oligomers and polymers have been synthesized and characterized by a number of methods. The absorption maxima of the neutral materials in solution fall in the range of 327–358 nm. An X-ray diffraction study of the di(fluorenyl)isoquinoline model compound shows significant twisting of the fluorene cores relative to the isoquinoline linker in the solid state. Conversion of the model compounds and polymers to a cationic form by *N*-alkylation generated the corresponding isoquinolininum salts with red shifted absorption maxima. The absorption maxima of the conjugated polycations fall in the range of 392–405 nm. Thus, the optical properties of isoquinoline based model compounds and polymers can be tuned by *N*-alkylation, an aspect that increases the attractiveness of *N*-methylated polymers for use as electron transport layer in OLEDs.

Acknowledgements

The authors acknowledge generous financial support from the Department of Science and Technology, New Delhi, India and the Max Planck Society, Germany. We thank Dr. S. K. Dhawan and Dr. Ritu Srivastava, National Physical Laboratory, New Delhi for extending their laboratory facilities.

References

[1] C.J. Tonzola, M.M. Alam, S.A. Jenekhe, Macromolecules 38 (2005) 9539–9547.

[2] C.J. Tonzola, M.M. Alam, B.A. Bean, S.A. Jenekhe, Macromolecules 37 (2004) 3554–3563.
[3] S.A. Jenekhe, L. Lu, M.M. Alam, Macromolecules 34 (2001) 7315–7324.
[4] C.G. Bangcuyo, M.E. Rampey-Vaughn, L.T. Quan, S.M. Angel, M.D. Smith, U.H.F. Bunz, Macromolecules 35 (2002) 1563–1568.
[5] X. Zhang, D.M. Kale, S.A. Jenekhe, Macromolecules 35 (2002) 382–393.
[6] A.P. Kulkarni, Y. Zhu, S.A. Jenekhe, Macromolecules 38 (2005) 1553–1563.
[7] Y. Cheng, L. Chen, X. Zou, J. Song, Z. Wang, Polymer 47 (2006) 435–440.
[8] M. Jonforsen, T. Johansson, O. Inganaes, M.R. Andersson, Macromolecules 35 (2002) 1638–1643.
[9] P.-I. Lee, S.L.-C. Hsu, J. Polym. Sci., Part A: Polym. Chem. 45 (2007) 1492–1498.
[10] T. Yamamoto, B.-L. Lee, H. Hayashi, N. Saito, T. Maruyama, Polymer 38 (1997) 4233–4239.
[11] D.-J. Liaw, K.-L. Wang, S.P. Pujari, Y.-C. Huang, B.-C. Tao, M.-H. Chen, K.-R. Lee, J.-Y. Lai, Dyes Pigm. 82 (2009) 109–117.
[12] H. Yun, T.K. Kwei, Y. Okamoto, Macromolecules 30 (1997) 4633–4638.
[13] W.Y. Huang, H. Yun, H.S. Lin, T.K. Kwei, Y. Okamoto, Macromolecules 32 (1999) 8089–8093.
[14] T. Yamamoto, N. Hayashida, React. Funct. Polym. 37 (1998) 1–17.
[15] D. Izuhara, T.M. Swager, J. Mater. Chem. 21 (2011) 3579–3584.
[16] D. Izuhara, T.M. Swager, J. Am. Chem. Soc. 131 (2009) 17724–17725.
[17] S.A. Jenekhe, X. Zhang, X.L. Chen, V.-E. Choong, Y. Gao, B.R. Hsieh, Chem. Mater. 9 (1997) 409–412.
[18] X. Zhang, A.S. Shetty, S.A. Jenekhe, Macromolecules 32 (1999) 7422–7429.
[19] X. Zhang, S.A. Jenekhe, Macromolecules 33 (2000) 2069–2082.
[20] A.K. Agrawal, S.A. Jenekhe, Macromolecules 24 (1991) 6806–6808.
[21] A.K. Agrawal, S.A. Jenekhe, Macromolecules 26 (1993) 895–905.
[22] H. Krueger, S. Janietz, D. Sainova, A. Wedel, Macromol. Chem. Phys. 204 (2003) 1607–1615.
[23] T. Kanbara, N. Saito, T. Yamamoto, K. Kubota, Macromolecules 24 (1991) 5883–5885.
[24] T. Kanbara, T. Yamamoto, Macromolecules 26 (1993) 1975–1979.
[25] R. Singh, A.S. Hay, Macromolecules 24 (1991) 2643–2646.
[26] Y. Cheng, J. Song, X. Zou, S. Zhang, Y. Liu, H. Huang, Polymer 47 (2006) 6598–6605.
[27] Y.-J. Su, H.-L. Huang, C.-L. Li, C.-H. Chien, Y.-T. Tao, P.-T. Chou, S. Datta, R.-S. Liu, Adv. Mater. (Weinheim, Ger.) 15 (2003) 884–888.
[28] E. Holder, B.M.W. Langeveld, U.S. Schubert, Adv. Mater. (Weinheim, Ger.) 17 (2005) 1109–1121.
[29] Z. Hu, C. Luo, L. Wang, F. Huang, K. Zhu, Y. Wang, M.-X. Zhu, W.-G. Zhu, Y. Cao, Chem. Phys. Lett. 441 (2007) 277–281.
[30] Z.Q. Gao, Z.H. Li, P.F. Xia, M.S. Wong, K.W. Cheah, C.H. Chen, Adv. Funct. Mater. 17 (2007) 3194–3199.
[31] G. Klaerner, R.D. Miller, Macromolecules 31 (1998) 2007–2009.
[32] S.H. Lee, T. Tsutsui, Thin Solid Films 363 (2000) 76–80.
[33] S. Setayesh, A.C. Grimsdale, T. Weil, V. Enkelmann, K. Mullen, F. Meghdadi, E.J. List, G. Leising, J. Am. Chem. Soc. 123 (2001) 946–953.
[34] W.-L. Yu, J. Pei, W. Huang, A.J. Heeger, Adv. Mater. (Weinheim, Ger.) 12 (2000) 828–831.
[35] D. Neher, Macromol. Rapid Commun. 22 (2001) 1365–1385.
[36] M.T. Bernius, M. Inbasekaran, J. O'Brien, W. Wu, Adv. Mater. (Weinheim, Ger.) 12 (2000) 1737–1750.
[37] U. Scherf, E.J.W. List, Adv. Mater. (Weinheim, Ger.) 14 (2002) 477–487.
[38] R. Scaria, K. Muellen, J. Jacob, Polymer 51 (2010) 5705–5711.
[39] N.N. Barashkov, H.J. Olivos, J.P. Ferraris, Synth. Met. 90 (1997) 41–47.
[40] W.D. Brown, A.-H. Gouliaev, Synthesis (2002) 83–86.
[41] R. Guentner, T. Farrell, U. Scherf, T. Miteva, A. Yasuda, G. Nelles, J. Mater. Chem. 14 (2004) 2622–2626.
[42] J. Pina, J. Seixas de Melo, H.D. Burrows, F. Galbrecht, A. Bilge, C.J. Kudla, U. Scherf, J. Phys. Chem. B 112 (2008) 1104–1111.
[43] M. Ranger, D. Rondeau, M. Leclerc, Macromolecules 30 (1997) 7686–7691.
[44] Y. Geng, S.W. Culligan, A. Trajkovska, J.U. Wallace, S.H. Chen, Chem. Mater. 15 (2003) 542–549.
[45] G.M. Sheldrick, Acta Crystallogr. Sect. A 64 (2008) 112–122.
[46] P. Coppens, L. Leiserowitz, D. Rabinovich, Acta Crystallogr. 18 (1965) 1035–1038.
[47] G. Saini, J. Jacob, SP. Senanayak, KS. Narayan, Polym. Bull. (Heidelberg, Ger.) doi:10.1007/s00289-010-0417-4.
[48] Y. Nagao, K. Hirota, M. Tokumaru, K. Kozawa, Heterocycles 73 (2007) 593–602.
[49] H.K. Fun, A. Usman, I.A. Razak, S. Chantrapromma, T.K. Sarkar, S. Basak, N. Panda, Acta Crystallogr., Sect. E 58 (2002) O215–O217.
[50] F. Durola, J.P. Sauvage, O.S. Wenger, Helv. Chim. Acta 90 (2007) 1439–1446.
[51] N. Haider, K. Mereiter, R. Wanko, Heterocycles 41 (1995) 1445–1459.
[52] A.K. Agrawal, S.A. Jenekhe, Chem. Mater. 8 (1996) 579–589.
[53] J.K. Politis, M.D. Curtis, Y. He, J. Kanicki, Macromolecules 32 (1999) 2484–2489.
[54] W.H. Melhuish, J. Phys. Chem. 65 (1961) 229–235.
[55] B. Strehmel, H. Seifert, W. Rettig, J. Phys. Chem. B 101 (1997) 2232–2243.